THE ONDULATOR AS A SOURCE OF ELECTROMAGNETIC RADIATION

D. F. ALFEROV, Yu. A. BASHMAKOV, K. A. BELOVINTSEV, E. G. BESSONOV, and P. A. CHERENKOV

P. N. Lebedev Physical Institute, Moscow, U.S.S.R.

(*Received September 15, 1978*)

The progress in various fields of natural sciences is closely connected with the development and utilization of new sources of electromagnetic radiation. Wide prospects are offered if ondulatory radiation sources are used in practice. Both the ondulator and synchrotron radiation are capable of covering a wide spectral range, from submillimeter waves to hard γ-radiation. Ondulatory radiation differs from the synchrotron radiation by higher intensity, directivity, monochromaticity and degree of polarization. There is also a possibility of operational changes in polarization modes of ondulatory radiation. Basic consequences of ondulatory-radiation theory are considered here. The requirements of the parameters of ondulators and the characteristics of charged-particle beams are discussed. Some experiments on electron radiation in a magnetic ondulator installed in a straight section of a synchrotron orbit are described.

INTRODUCTION

As a rule, the development and utilization of electromagnetic radiation sources with improved parameters stimulate the progress in various fields of natural sciences. From this point of view, an obvious interest to the ondulatory radiation (OR) has been growing in recent years. The OR source includes a relativistic charged-particle accelerator or storage ring and an ondulator. The ondulator is commonly considered as a unit, where under the effect of an external electromagnetic field the relativistic charged particles are forced to oscillate periodically relative to the uniformly moving center. The oscillatory travel of particles is accompanied by electromagnetic radiation at Doppler frequencies.

V. L. Ginsburg proposed in 1947 the use of fast-particle radiation in practice.[1] In the early 1950's H. Motz,[2] K. Landeker,[3] and others worked on development and realization of this idea. At the same time, H. Motz introduced the term *ondulator* (from the French, *ondulation* or wiggling).† The hope to obtain sufficient radiation power was due to the use of an electron beam formed as a series of the bunches with length of the order of the radiated wavelength. H. Motz and collaborators[4] used the output electron beam of a linear accelerator at an energy of 5 MeV and a current of 10 mA per pulse. They achieved generation of coherent radiation in the millimeter wavelength range at a pulse power about 1 W, the magnetic field in ondulator harmonically changing in magnitude. The non-coherent OR in the submillimeter and optical range of wavelengths was studied in Refs. 4 and 5. The electron sources here were linear resonance accelerators of energy 3 to 100 MeV. The OR from an electron beam extracted from a synchrotron at 3.6 GeV was experimentally studied in Ref. 6. Reference 7 discusses the detection of induced radiation of relativistic electrons in the ondulator. Interest in the non-coherent radiation of particles in ondulators has grown as well with the increase of research work on applications of synchrotron radiation of ultrarelativistic particles.

The use of electrons at energies up to some hundreds of GeV can make it possible (due to OR) to cover the entire frequency band from submillimeter wavelengths to the hard γ-radiation (inclusive). Compared to synchrotron radiation (SR), the OR has higher intensity, directivity, monochromaticity, degree of polarization and the capability of operational change of polarization mode. Several experiments have been made to date on electron radiation in a magnetic ondulator installed into a straight section of the orbit at the "Pakhra" synchrontron.[8,39] An installation of ondulators is being planned as well in the straight sections of storage rings, both in presently operating

† More recently these systems have been called "wigglers".

ones[9,10] and in storage rings projected as dedicated sources of synchrotron radiation.[11–13] It is promising to consider use of ondulators from high-energy electron beams obtained at the largest proton accelerators.[14]

The OR theory is developed in Refs. 15–26, 40. Some features of OR are considered in Refs. 27–29.

The basic properties of non-coherent OR, possible modifications of ondulators, OR source characteristics for helical ondulators and their applications are considered in the present work. Some experiments on observation of ondulatory radiation from a synchrotron orbit are also reviewed.

I BASIC PROPERTIES OF OR

Let us consider the radiation of an ultrarelativistic particle, where $\gamma = (E/mc^2) \gg 1$ and E and m are the energy and the particle mass, which performs forced oscillations at frequency Ω while traveling along the ondulator axis. The radiation of such a particle is mainly concentrated in a small cone of angle $\Delta\theta \sim 1/\gamma$ relative to its velocity direction. The radiation characteristics depend significantly on the relation between the size of interval and the maximal bending angle α of the particle velocity vector in the ondulator field. In the case of a sinusoidal trajectory,

$$\alpha = \frac{eH_m\lambda_0}{\pi mc^2\gamma}, \tag{1}$$

where $\lambda_0 = 2\pi\beta_{\|}\, c/\Omega$ is the period of particle oscillation $\beta_{\|}\, c$ is the particle velocity along the ondulator axis, averaged over the period of the ondulator, and H_m is the magnetic-field amplitude. Note that the relation of α to the interval

$$\Delta\theta\left(\frac{\alpha}{\Delta\theta} = \alpha\gamma\right)$$

is not dependent on the particle energy.

If the bending angle of the particle velocity vector is much less than $\Delta\theta(\alpha\gamma \ll 1)$, the radiation of the entire trajectory will be in a small interval of the angle around the direction of travel. In this case, the radiation of a particle is similar to that of a rapidly moving dipole. For harmonic oscillation, the radiation frequency, determined by the Doppler effect, is

$$\omega_1 = \frac{\Omega}{1 - \beta_{\|} \cos\theta}, \tag{2}$$

where θ is the angle between the observation direction and the ondulator axis. It follows that for a particle at relativistic longitudinal velocity $(1 - \beta_{\|} \ll 1)$, the radiation frequency ω_1 observed at small angles relative to the ondulator axis considerably exceeds the oscillation frequency Ω of the particle.

The relation (2), which is true for an infinitely long ondulator single-valuedly combines the radiation frequency ω_1 and the observation angle θ. In the approximation under consideration, only the first harmonic at the maximum frequency $\omega_{1m} = 2\Omega\gamma^2$ is radiated.

In case of non-harmonic oscillations (for example, a particle traveling in a piecewise-constant magnetic field), an uneven harmonic radiation takes place. An increase of the relative length of intervals free from magnetic field in an ondulator results in an increase of the highest-harmonic radiation.[15,16]

The radiation spectrum form in a dipole approximation $(\alpha\gamma \ll 1)$ is specific for each ondulator and does not depend on the magnitude of the magnetic field.[15,16,19] The spectral intensity of OR spectrum sharply falls at frequencies greater than the first harmonic. This property allows one, in principle, to make threshold detection of particles.[15,16]

In a real case, the ondulator has finite length $L = K\lambda_0$, where K is the number of periodicity elements, so the radiation-pulse duration at an observation point is also finite. This results in widening the radiation spectrum line in the direction on θ by[19]

$$\frac{\Delta\omega}{\omega_k} \simeq \frac{1}{kK}, \tag{3}$$

where $\omega_k = k\omega_1$ and k is the harmonic number.

The intensity of a spectral line is proportional to the number of periodicity elements K. Note that at a fairly large $K(K > 10)$, the radiation spectrum integrated over all directions differs slightly from the radiation spectrum in an infinitely long ondulator.[15,16]

When the condition of dipole radiation is violated, the oscillation amplitude increases and the mean velocity of a particle along the ondulator axis decreases. In a coordinate system where the particle is on the average at rest, its travel becomes relativistic and, as a consequence, radiation in the highest harmonics is increased. In this case, the OR spectrum depends on the electromagnetic-field magnitude. With the decrease of longitudinal velocity $\beta_{\parallel} c$, the radiation frequency of the kth-harmonic decreases compared with the dipole approximation.

In the maximum permissible case, the $\alpha\gamma \gg 1$ radiation at an observation point is defined only by trajectory portions where the particle velocity vector bends at an angle $\sim 1/\gamma$ relative to the observation direction, which is $\sim 2/\alpha\gamma$ of the whole ondulator length. The OR spectrum integrated over angles resembles in its form the SR spectrum, but at a fixed angle, the spectrum distribution is different because the interval between the neighboring OR harmonics is rather larger than that in the SR spectrum. The polarization OR characteristics also differ considerably from those of SR.[19,23]

For an ondulator in a straight section of a storage ring, the particle radiation intensity per unit solid angle near the ondulator axis is $2K$ times higher than the SR intensity in the same solid angle with the same magnetic fields on the storage ring orbit and in the ondulator.

An important feature of the ondulator is that there is available an optimal field value of $\alpha\gamma \simeq 1$, when the radiation intensity on the first harmonic per unit solid angle is maximum.[15,16,19]

The optimal field magnitude depends in each case on the type of particle trajectory in the ondulator. The trajectories can be divided into two classes, flat trajectories (the simplest case is a sinusoidal trajectory) and trajectories similar to a helix (helical trajectories). The radiation characteristics significantly differ.

In the first case, the radiation of a particle in the direction along the ondulator axis consists of a set of harmonics and is fully polarized at a given frequency irrespective of field magnitude. When observed in an arbitrary direction, only the orientation of the OR polarization plane changes. It essentially differs from SR. In case of helical movement in direction $\theta = 0$, only the first harmonic polarized over the circle radiates.

When the fields are near the optimal value, the main part of radiation intensity is in the first harmonic. In this case, the halfwidth of the OR spectrum integrated over the angles is much less than that of SR. The above circumstance and the linear nature of the spectrum in the observation direction simplify considerably the task of preliminary monochromatization and filtration of radiation. If the condition of optimal generation if followed, the spectral OR intensity at ω_{1m} rather exceeds the SR spectral intensity at the same frequency.

The spectral and angular-radiation characteristics for both types of travel are considered in detail in Refs. 19, 21–23. The characteristics of ondulator magnetic field which are responsible for such trajectories are also given.

II MAIN TYPES OF ONDULATORS

Let us consider the main types of ondulators.

1) The magnetic ondulator is a series of magnets located along the axis of the instrument in such a way that the magnetic-field direction changes by an angle of $2\pi/n$, where $n = 2, 3, \ldots$, is an integer, when one moves to the next magnet. In such systems, a transverse magnetic field is formed. The magnitude and direction of the field vary periodically along the ondulator axis.

The magnetic ondulator with alternating-sign field ($n = 2$) proposed by H. Motz[4] consists of a set of steel pieces fitted between the poles of magnetron magnets. An analogous system of pole pieces fitted in the gap of an electromagnet was used in Refs. 4, 5 and 6. Magnetic ondulators with flat single-loop windings are now developed and manufactured.[31,32] Super-conducting magnetic ondulators are available with fields of $H = 4$ to 5 T.[8–13] In a magnetic ondulator with alternating-sign field, the particle trajectory is in a single plane. If the magnetic field of the ondulator is described by an uneven function, the particle radiation will be then linearly polarized. In particular, it is possible to design an ondulator so that its field will vary as

$$\mathbf{H} = \mathbf{i} H_m \sin \frac{2\pi}{\lambda_0} z, \tag{4}$$

where $\mathbf{i}$ is a unit vector perpendicular to the long axis of the ondulator z. $n \geq 3$ corresponds[17,30] to a magnetic ondulator forming a turning piecewise-constant field.

2) The simple helical ondulator is a cylindrical coil which consists of two similar solenoids with winding pitch λ_0. The solenoids form a double helix carrying current in opposite directions, which shift relatively to each other by a half pitch.[19] The magnetic field near the ondulator axis varies as

$$\mathbf{H} = \mathbf{i} H_{\perp} \sin \frac{2\pi}{\lambda_0} z \mp \mathbf{j} H_{\perp} \cos \frac{2\pi}{\lambda_0} z, \tag{5}$$

where the sign $(-)$ or $(+)$ reflects the turning direction of the magnetic field defined by the direction of winding of the solenoids and the unit vectors $\mathbf{i}$ and $\mathbf{j}$ are along the x and y axes respectively.

TABLE I

Maximum photon energy as a function of particle energy

E (GeV)	1	3	10	30	10^2	3×10^2	10^3
$\varepsilon_{\gamma 1 m}$(MeV)	5×10^{-4}	4.5×10^{-3}	5×10^{-2}	0.45	5	45	5×10^2

The motion of a particle in this case is helical. The radiation in the optimal generation mode is characterized by a high degree of circular polarization.

A superconducting modification of a simple helical ondulator 5.2 m long with a period of $\lambda_0 = 3.2$ cm and magnetic field amplitude $H_\perp = 0.24$ T was used in experiments with induced OR.[7]

3) The universal helical ondulator is a system of two concentrically located simple helical ondulators with equal pitch and opposite direction of winding.[25] When current is transmitted through the first or the second coil one can change the rotation direction of magnetic field and, correspondingly, the radiation polarization. If the current is passed through the conductors of both coils, a harmonic field from Eq. (4) (where $H_m = 2H_\perp$) can be excited. An alteration of the current direction in one of the coils results in a bending of the field vector and, correspondingly, of the radiation polarization plane by 90°. A smooth alteration of the magnetic field direction can be made by bending of one of the coils. Thus, a universal helical ondulator makes it possible to change the OR polarization mode in operation.

A common feature of the above-mentioned ondulators is the periodicity in space of the magnetic fields produced. The particle-oscillation frequency in such ondulators is determined by the period of magnetic-field alteration λ_0 and the particle velocity $\beta_\parallel c$

$$\Omega = \frac{2\pi\beta_\parallel c}{\lambda_0} \tag{6}$$

These ondulators may be installed at the output of linear accelerators,[7] in the channels of proton-synchrotron electron beams,[14] or in straight sections of synchrotrons or storage rings.[8–13,30,31] The aperture of the ondulator should exceed the transverse charged-particle beam dimensions at the location of ondulator installation. Starting from this condition and taking into account the practicalities of modern engineering, one can show that to obtain magnetic fields exceeding 0.1 T, the minimal period of ondulator should be $\lambda_0 \simeq 1$ cm. The utilization of such ondulators will permit achievement of an intense flux of polarized electromagnetic radiation in a wide spectrum range. The OR frequency is altered by particle-energy change.

The dependence of the maximum energy of photons $\varepsilon_{\gamma 1 m}$ (2) radiated in the first harmonic in a small-field ondulator with $\lambda_0 = 2$ cm upon the energy of electrons E is given in Table I.

Electron energies near 10 GeV are obtained in modern linear accelerators, synchrotrons and storage rings. The energies higher than 10^2 GeV are obtained in electron beams at the largest proton synchrotrons.

4) In ondulators with solenoids and quadrupole lenses,[15,16,18] unlike the above ondulators, the oscillation frequency Ω decreases with particle-energy increase. With present-day technology of developing magnetic fields and gradients, one may achieve too large a period of the ondulator $\lambda_0 = 2\pi\beta_\parallel c/\Omega$ corresponding to this frequency. At this time a value of $\lambda_0 \simeq 10^2$ cm can be achieved at an electron energy of 1 GeV.

5) Electromagnetic waves.[2,3,17,23,33] When an electromagnetic wave travels counter to a particle beam, the particle oscillates at frequency

$$\Omega = \omega_w(1 + \beta_\parallel), \tag{7}$$

where ω_w is the wave frequency. According to (6) and (7), ondulators based on electromagnetic waves have an equivalent periodicity-element length

$$\lambda_0 = \frac{\lambda_w}{1 + \beta_\parallel}, \tag{8}$$

where $\lambda_w = 2\pi c/\omega_w$ is the wavelength of the electromagnetic wave.

The radiation characteristics in a field with a plane electromagnetic wave practically coincide with the radiation characteristics in ondulators having harmonic fields.[23] The main advantage of ondulators with electromagnetic waves is the short equivalent periodicity element length λ_0, and as a consequence, more hardness of the radiation generated. The sources of electromagnetic waves may be, for example, masers, lasers and sources of both non-coherent[34] and coherent[26] OR.

6) Crystals. The OR can be generated by particles traveling along a crystal atom chain[23] or channeling interplanarly and axially.[35]

The minimal effective period of an ondulator made on a crystal base equals the lattice spacing and is within the limits $\lambda_0 \simeq 2$ to 5 Å. In the case of channeling, $\lambda_0 > 10^2$ to 10^3 Å, and as a rule, is much less than that in magnetic or helical ondulators. As in the case of a quadrupole lens, it is determined by the value of electric-field gradient in the crystal and the energy of the particle. The characteristics of particle radiation in quadrupole field are considered in Refs. 15 and 35.

Particle radiation in a crystal is very hard. For example, at $E = 10$ MeV, $\lambda_0 = 3$ Å, the energy of radiated quantum $\varepsilon_{\gamma 1}$ is comparable with the electron energy. At $\varepsilon_{\gamma 1} > E/2$, the spectrum and polarization characteristics of particle radiation are deteriorating. So, using electrons at some GeV, the magnitude λ_0 is selected to exceed the period of lattice. This is achieved by the corresponding choice of the angle between the electron velocity and crystal axes.

The polarization of radiation is linear when an electron travels parallel to the chain of atoms located on a single straight line or channels interplanarly. The radiation possesses significant circular polarization[36] when the particle motion is parallel to the helical axis of a crystal having helicoidal structure or channels axially if the trajectory is helical.

To obtain polarized quasi-monochromatic γ-quanta, the crystals are fitted in electron beams at the output of linear accelerators or in synchrotron straight sections near the equilibrium orbit.

3 CHARACTERISTICS OF NON-COHERENT OR SOURCES BASED ON HELICAL ONDULATORS

Let us consider, as an example, particle radiation in a standard (normal) helical ondulator. The motion of a particle in the field (5) formed by such an ondulator, with proper selection of initial conditions, is helical.[19,22,23]

$$\mathbf{r}(t) = \mathbf{i}R \cos \Omega t + \mathbf{j}R \sin \Omega t + \mathbf{k}\beta_{\|}\, ct, \tag{9}$$

where $\mathbf{k}$ is the unit vector along the z axis, $R = (\lambda_0/2\pi)(\beta_\perp/\beta_\|)$ is the helical radius, and $\beta_\perp c$ is the projection of the particle velocity on the surface perpendicular to the helical axis. The values $\beta_\perp$ and $\beta_\|$ are defined by the magnetic-field amplitude and the particle energy

$$\beta_\perp = \frac{eH_\perp \lambda_0}{2\pi mc^2\gamma}, \qquad \beta_\| = \beta\sqrt{1 - \left(\frac{\beta_\perp}{\beta}\right)^2}. \tag{10}$$

The spectral angular radiation intensity of a particle traveling helically in an ondulator with periodicity elements K is[23]

$$\frac{dI}{d\omega dO} = \frac{3I}{4\pi^3 K\Omega\gamma^4} \sum_{k=1}^{\infty} \times \frac{\sin^2 \pi K k[(\omega - \omega_k)/\omega_k]}{k^2[(\omega - \omega_k)/\omega_k]^2} \left(\frac{\omega}{\Omega}\right)^2 F_k(\theta) \tag{11}$$

where

$$I = 2e^2\Omega^2 P_\perp^2 \gamma^2/3c \tag{12}$$

is the full particle-radiation intensity, $P_\perp = \beta_\perp \gamma$ is the scaled transverse particle momentum,

$$\omega_k = \frac{k\Omega}{1 - \beta_\| \cos\theta} = k\omega_1 \tag{13}$$

$(k = 1, 2, 3, \ldots,)$ is the number of the harmonic radiated,

$$F_k(\theta) = T_k'^2(k\kappa) + \left(\frac{\cos\theta - \beta_\|}{1 - \beta_\| \cos\theta}\right)^2 \frac{1}{\kappa^2} T_k^2(k\kappa), \tag{14}$$

$\kappa = \beta_\perp \sin\theta/(1 - \beta_\| \cos\theta)$, and T_k, T_k' are the Bessel function and its derivative.

From (11), one can see that the particle radiation in the ondulator at angle θ relative to the helical axis is concentrated at frequencies (13), with the half-width of the line (3).

If $K \gg 1$, the angular and spectral particle radiation distributions are given by[25]

$$\frac{dI}{dO} = \sum_{k=1}^{\infty} \frac{dI_k}{dO} = \frac{3I}{4\pi\gamma^4} \frac{F(\theta)}{(1 - \beta_\| \cos\theta)^3}, \tag{15}$$

$$\frac{dI}{d\omega} = \sum_{k=1+k'}^{\infty} \frac{dI_k}{d\omega} = \frac{3I\omega}{2\beta_\| \Omega^2\gamma^4} F(\omega), \tag{16}$$

where

$$F(\theta) = \sum_{k=1}^{\infty} k^2 F_k(\theta) = \frac{4 + 3\kappa^2}{16(1 - \kappa^2)^{5/2}} + \left(\frac{\cos\theta - \beta_{\|}}{1 - \beta_{\|}\cos\theta}\right)^2 \frac{4 + \kappa^2}{16(1 - \kappa^2)^{7/2}},$$

$$F(\omega) = \sum_{k=1+k'}^{\infty} F_k[\theta_k(\omega)], \qquad k' = E[\omega(1 - \beta_{\|})/\Omega],$$

$E(x)$ is the integer of x, and

$$\theta_k(\omega) = \cos^{-1}\left[\frac{1}{\beta_{\|}}\left(1 - \frac{k\Omega}{\omega}\right)\right].$$

We shall describe the optimal generation conditions when the first harmonic of spectral-angular and angular radiation intensity is maximized (see section 1). According to (11), (14) and (15) the maximum of the first harmonic of the angular intensity is at $P_{\perp} = 1/\sqrt{2}$, and that of the spectral angular intensity is at[10,19] $P_{\perp} = 1$. The optimal magnetic-field magnitude in the first case is

$$H_{\perp\,\mathrm{opt}} = \frac{\pi\sqrt{2}mc^2}{e\lambda_0}. \tag{17}$$

The radiation of a particle traveling on a helical trajectory is in the general case elliptically polarized. The ratio of the half-axes of polarization ellipse of the radiation kth harmonic is[23]

$$\frac{q_{1k}}{q_{2k}} = \frac{\beta_{\perp}\sin\theta T_k'(k\kappa)}{(\beta_{\|} - \cos\theta)T_k(k\kappa)}. \tag{18}$$

The degree of kth harmonic circular polarization ((+) right, (−) left) of radiation is

$$P_k = \frac{2q_{1k}q_{2k}}{q_{1k}^2 + q_{2k}^2} = \frac{F_{k+} - F_{k-}}{F_k}, \tag{19}$$

where

$$F_{k\pm} = \frac{1}{2}\left[T_k'(k\kappa) \pm \frac{\cos\theta - \beta_{\|}}{(1 - \beta_{\|}\cos\theta)}\cdot\frac{1}{\kappa}T_k(k\kappa)\right]^2.$$

The functions $F_{k\pm}$ are related to the F_k ratio $F_k = F_{k+} + F_{k-}$. They define the radiation intensity of waves with right and left circular polarization

$$\frac{dI_{k\pm}}{dO} = \frac{1 \pm P_k}{2}\frac{dI_k}{dO} = \frac{F_{k\pm}}{F_k}\frac{dI_k}{dO} = \frac{3I}{4\pi\gamma^4}\frac{k^2 F_{k\pm}}{(1 - \beta_{\|}\cos\theta)^3} \tag{20}$$

The degree of circular polarization averaged over all harmonics of the radiation at frequency ω and radiation observed at an angle θ are correspondingly

$$P(\omega) = \frac{1}{dI/d\omega}\sum_{k=1+k'}^{\infty}\left(\frac{dI_{k+}}{d\omega} - \frac{dI_{k-}}{d\omega}\right) = \frac{1}{F(\omega)}\sum_{k=1+k'}^{\infty}[F_{k+}(\omega) - F_{k-}(\omega)],$$

$$P(\theta) = \frac{1}{dI/dO}\sum_{k=1}^{\infty}\left(\frac{dI_{k+}}{d\theta} - \frac{dI_{k-}}{d\theta}\right) = \frac{\tilde{F}(\theta)}{F(\theta)}, \tag{21}$$

where

$$\tilde{F}(\theta) = \sum_{k=1}^{\infty} k^2(F_{k+} - F_{k-}) = \frac{\cos\theta - \beta_{\|}}{1 - \beta_{\|}\cos\theta}\cdot\frac{1}{\kappa}\sum_{k=1}^{\infty} k^2 T_k(k\kappa)T_k'(k\kappa).$$

Here the approximate formula

$$\sum_{k=1}^{\infty} k^2 T_k(k\kappa)T_k'(k\kappa) \simeq \frac{2 + \kappa^2}{8(1 - \kappa^2)^3}$$

is quite convenient, which at $\kappa < 0.8$ has an accuracy of $\simeq 10^{-3}$.

In the relativistic case $1 - \beta \ll 1$, Eqs. (11)–(21) may be simplified if the longitudinal particle velocity is relativistic as well, if $1 - \beta_{\|} \ll 1$. In this case, according to (11)–(13), the main part of the radiated energy is in the region of small angles $\Delta\theta \sim \beta_{\perp} \ll 1$ and high frequencies $\omega_k \sim 2k\Omega\gamma^2$.

Introduce a dimensionless frequency and an angle accordingly to the relations

$$\xi = \frac{\omega}{2\Omega\gamma^2}, \qquad \vartheta = \theta\gamma \tag{22}$$

Then the radiated frequency, the equations for radiation intensity (11), (15), (16) and the inherent functions may be written as

$$\xi_k = \xi_{km}\frac{1 + P_{\perp}^2}{1 + P_{\perp}^2 + \vartheta^2}, \qquad \xi_{km} = \frac{k}{1 + P_{\perp}^2}, \tag{23}$$

$$\frac{dI}{d\xi dO} = \frac{6I\gamma^2}{\pi^3 K}\sum_{k=1}^{\infty}\frac{\sin^2\pi Kk[(\xi - \xi_k/\xi_k)]}{k^2[(\xi - \xi_k/\xi_k)]^2}\xi^2 F_k(\theta), \tag{24}$$

$$\frac{dI}{dO} = \frac{6I\gamma^2}{\pi}\frac{F(\theta)}{(1 + P_{\perp}^2 + \vartheta^2)^3}, \tag{25}$$

$$\frac{dI}{d\xi} = 6I\xi F(\xi),$$

$$\kappa(\vartheta) = \frac{2\vartheta P_\perp}{1 + P_\perp^2 + \vartheta^2},$$

$$\kappa(\xi) = \frac{2P_\perp}{k}\sqrt{\xi[k - \xi(1 + P_\perp^2)]}$$

$$\frac{\cos\theta - \beta_\parallel}{1 - \beta_\parallel\cos\theta} = \frac{1 + P_\perp^2 - \vartheta^2}{1 + P_\perp^2 + \vartheta^2}. \tag{26}$$

We show in Figures 1–5 the basic characteristics of OR calculated from (21), (25), (26). In Figure 3 one can see that at the optimal magnetic field, the main part of the radiated energy is concentrated in the vicinity of the direction $\vartheta = 0$ in a region of angular width $\Delta\theta \simeq 1/2\gamma$. In this region, $P > 95\%$ from Figure 4. The degree of circular polarization changes from $P = 1$ at $\vartheta = 0$ to $P = -1$ at $\vartheta \gg 1$. In the direction $\vartheta = \sqrt{1 + P_\perp^2}$, $P = 0$. In this direction the radiation is linearly polarized. With an increase of the magnetic-field amplitude, the maximum of radiation intensity is shifted to larger angles (see Figure 5). From Figures 4 and 3 it follows that at the optimal field, 50% of radiated energy is in the first harmonic. The halfwidth of the spectrum near the maximal frequency corresponding to the first harmonic $\xi_{1m} = \frac{2}{3}$ is $\simeq 15\%$. With the optimal field, the degree of polarization changes from -1 to 0.8 in the frequency range $0 \leq \xi \leq \xi_m$ (Figure 2).

We have considered above the characteristics of the OR radiated by a single particle. We shall express the beam radiation intensity in an ondulator in terms of the beam current T and the radiation intensity of a single particle I

$$I_b = \frac{TK\lambda_0}{e\beta\ c} I \tag{27}$$

Substituting I_b for I in (24)–(26), one can determine all the characteristics of OR parallel to the

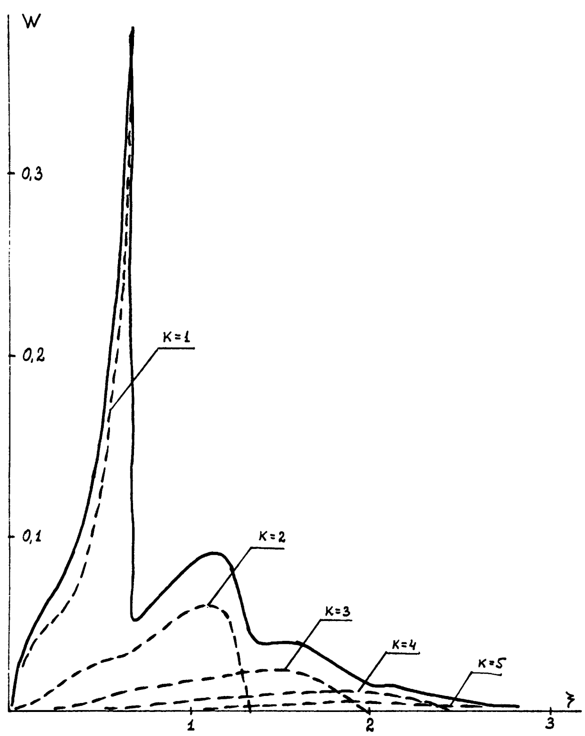

FIGURE 1 Spectral distribution of ondulatory radiation intensity at $P_\perp = 1/\sqrt{2}$; —— summed radiation, ---radiation in harmonics.

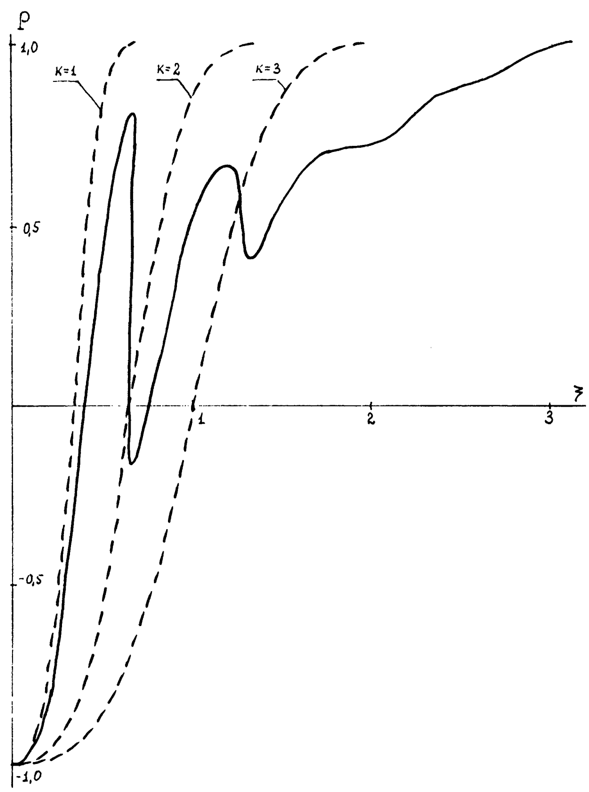

FIGURE 2 Spectral distribution of circular polarization degree of radiation at $P_\perp = 1/\sqrt{2}$; —— summed radiation, --- radiation in harmonics.

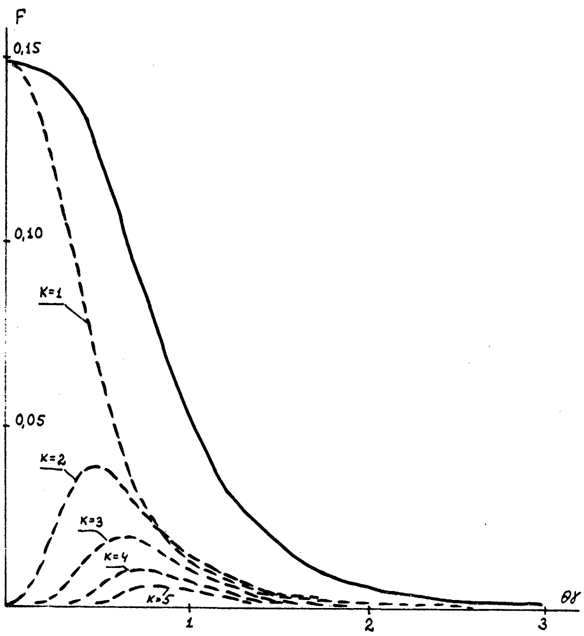

FIGURE 3 Angular distribution of ondulatory radiation intensity at $P_\perp = 1/\sqrt{2}$; ——summed radiation, --- radiation in harmonics.

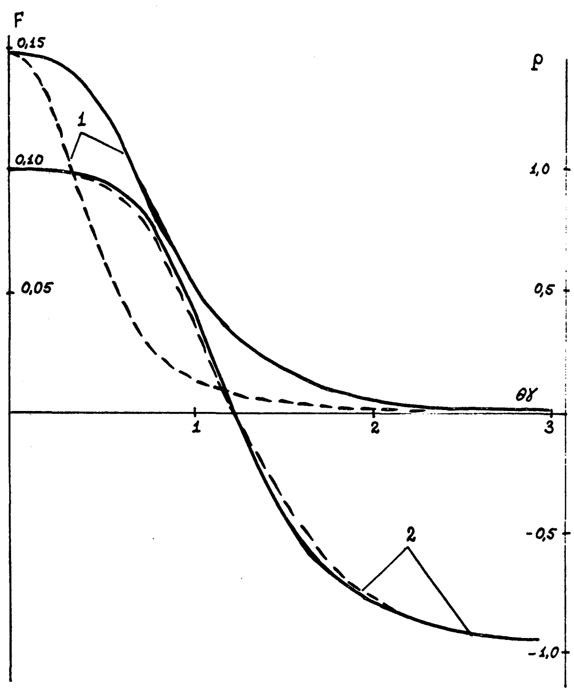

FIGURE 4 Angular distribution of radiation intensity (1) and circular polarization degree (2) at $P_\perp = 1/\sqrt{2}$; —— summed radiation, --- radiation in the first harmonic.

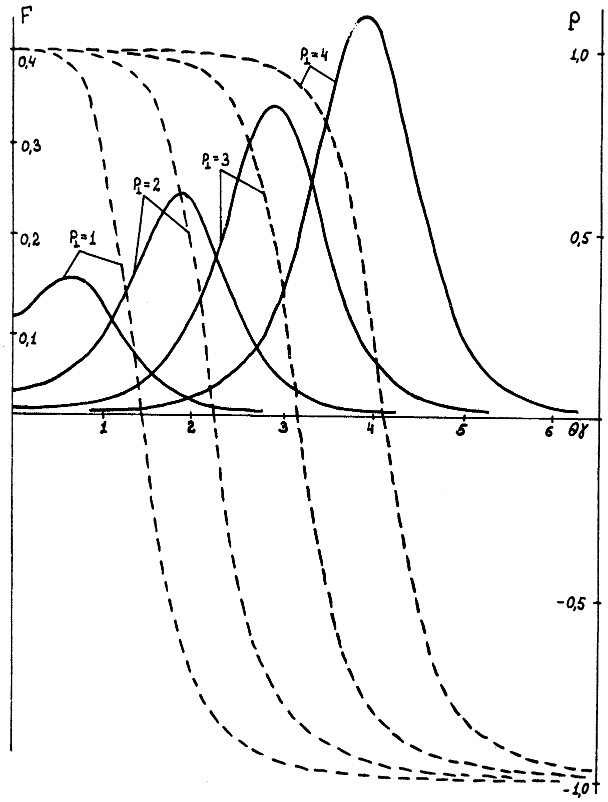

FIGURE 5 Angular distribution of ondulatory radiation intensity (——) and circular polarization degree (---) at different $P_\perp$.

particle beam. We can present Eq. (27) in a form suitable for practical calculations if we take $\beta_\parallel = 1$. Then

$$I_b(wt) = 3.3 \cdot 10^{-12} \gamma^2 H_\perp^2(0e) K \lambda_0(m) T(a) \quad (28)$$

The angular spread and transverse dimensions of the particle beam[10,23,37,40] considerably affect the characteristics of OR. To determine the OR properties of a particle beam with angular spread ϑ_b, one should replace ϑ^2 by $\vartheta^2 - \vartheta_b^2$ in Eqs. (23) through (26) and average over the spread in angle.

According to (13) and (23), the angular divergence of particles in a beam results in widening the spectral line (3) when observed in a given direction. Because of the angular spread, the natural OR line-width $\Delta\xi = \xi_{m1}/K$ in direction $\vartheta = 0$ will increase to

$$\Delta\xi_m = \xi_{m1} \frac{\vartheta_b^2}{1 + P_\perp^2 + \vartheta_b^2} \quad (29)$$

The width of the radiation spectral line will not change noticeably if

$$\vartheta_b \ll \vartheta_b' = \sqrt{(1 + P_\perp^2)/2K} \tag{30}$$

The angular spread ϑ_b results in an increase of OR angular divergence

$$\Delta\theta \simeq \frac{1}{\gamma}\sqrt{1 + P_\perp^2 + \vartheta_b^2} \tag{31}$$

and, correspondingly, to a decrease of angular intensity and the degree of circular polarization. At the same time, the OR spectral intensity integrated over all directions (26) depends only weakly on ϑ_b.

One may neglect the effect of particle-energy spread in a beam on the OR properties provided that

$$\frac{\Delta\gamma}{\gamma} \ll \frac{1}{K}, \tag{32}$$

this condition being fulfilled in actual accelerators.

The spectral brightness of the OR source, the spectral-angular intensity of radiation per unit area of visual surface of the source,

$$B(\xi, \theta) = \frac{dI_b}{d\xi d\theta}\Big/ S\cos\theta, \tag{33}$$

depends on the dimensions and angular spread of the beam. Here S is the source surface area.

For a cylindrical beam with radis a, and for $\theta \ll 1$,

$$S\cos\theta = \pi R_b^2 + \frac{2}{\gamma} L R_b \vartheta,$$

$$R_b^2 = a^2 + R^2 + \frac{L^2}{\gamma^2}\vartheta_b^2, \tag{34}$$

where R is the radius of the helical trajectory of a particle, and is the ondulator length. Notice that with fields near optimum or less, one may neglect the quantity R in (34) when compared with the beam radius. The beam radius cannot be neglected.

The angular spread ϑ_b and transverse dimensions of a beam depend on the magnetic-system parameters of the accelerator or storage ring. In these systems, the product $\varepsilon = a\vartheta_b/\gamma$, proportional to the emittance of the particle beam at energy E, remains constant. In this case, in the direction $\vartheta = 0$ the visible surface of the beam in the ondulator,

$$S = \frac{\pi}{\vartheta_b^2}\left[\varepsilon^2\gamma^2 + \left(\frac{L}{\gamma}\right)^2 \vartheta_b^4\right] \tag{35}$$

reaches a minimal value at

$$\vartheta_b = \vartheta_b'' = \gamma\sqrt{\frac{\varepsilon}{L}} \tag{36}$$

The spectral-angular intensity of an OR particle beam (32) essentially depends on the angular spread ϑ_b. If the particles in a beam are uniformly distributed over angles, the OR intensity at frequency ξ_{1m} in the direction $\vartheta = 0$ has the form according to (24) and (27)

$$\frac{dI_b}{d\xi dO}(\xi_{1m}, \theta) = \frac{1}{1 + (\vartheta_b/\vartheta_b')^2}\frac{I_b}{I}\frac{dI}{d\xi dO}(\xi_{1m}, \theta) \tag{37}$$

Substituting (35) and (37) in (33), we determine the dependence of the OR source brightness on an angular divergence of a beam.

$$B(\xi_{1m}, \theta) = \frac{1}{\pi\varepsilon L}\frac{x}{(1 + cx)(1 + x^2)} \times \frac{I_b}{I}\frac{dI}{d\xi d\theta}(\xi_{1m}, \theta), \tag{38}$$

where

$$x = \left(\frac{\vartheta_b}{\vartheta_b''}\right)^2, \quad c = \left(\frac{\vartheta_b''}{\vartheta_b'}\right)^2 = \frac{2\varepsilon\gamma^2}{\lambda_0(1 + P_\perp^2)}$$

From (38) it follows that the optimal value of angular spread with a maximal brightness is defined by the roots of the equation

$$2cx^3 + x^2 - 1 = 0 \tag{39}$$

With the condition $c \gg 1(\varepsilon \gg [(1 + P_\perp^2)\lambda_0]2\gamma^2)$, which is fulfilled in electron accelerators and storage rings at high energies, the solution of Eq. (39) has the form

$$x = \sqrt[3]{\frac{1}{2c}} \quad \text{or} \quad \vartheta_b = \sqrt[3]{\vartheta_b''^2 \cdot \vartheta_b' \cdot \tfrac{1}{2}}. \tag{40}$$

Then the spectral brightness of the OR source at ξ_{1m} in direction $\vartheta = 0$ is

$$B \simeq \frac{1 + P_\perp^2}{2\pi\varepsilon^2\gamma^2 K}\frac{I_b}{I}\frac{dI}{d\xi dO}. \tag{41}$$

In accordance with (37), the spectral-angular intensity of OR will decrease $1 + (\vartheta_b''/\vartheta_b')^{4/3}$ times compared with the radiation of a parallel beam. With a decrease of the beam angular spread to $\vartheta_b \simeq \vartheta_b'$, its effect on the value of the OR spectral-angular intensity becomes less noticeable, and the spectral brightness (38) decreases no more than twofold as compared with the maximum value.

From the above considerations, it follows that in electron storage rings designed as special sources of SR one should take into account long straight sections where angular particle spread in a beam is considerably decreased (a section with a high β function).[23] Putting a helical ondulator in such a straight section makes it possible to obtain intense strongly directional-polarized quasi-monochromatic electromagnetic radiation.

As an example, we consider radiation of an electron beam with angular spread $\vartheta_b \sim \vartheta_b'$ in a helical ondulator placed in a straight section of a storage ring.

Suppose the ondulator and storage ring have the parameters

$$\text{ondulator: } \lambda_0 = 2\text{ cm}, K = 10^2,$$

$$H_\perp = 0.38\text{ T}\left(\mathrm{P}_\perp = \frac{1}{\sqrt{2}}\right).$$

$$\text{storage ring: } E = 2\text{ GeV } (\gamma \simeq 4 \times 10^3),$$

$$T = 1a, H = 1\text{ T}, \varepsilon = 10^{-5}\text{ cm-rad.}$$

$$\vartheta_b = \vartheta_b' \simeq 0.1\ (\theta_b = 2.5 \times 10^{-5}),\ \vartheta_b'' \simeq 0.9.$$

In this case, a full OR intensity $I_b = 1.65$ kW is radiated, largely in an interval of angular width $\Delta\theta \simeq 3 \times 10^{-4}$ According to (37), the spectral-angular intensity of electron-beam radiation at frequency

$$\omega_{1m} (\hbar\omega_{1m} = 1.26\text{ keV}, \lambda_{1m} = 0.95\text{ Å})$$

is

$$\frac{dI_b}{d\omega dO} = 1.12 \times 10^{-7}\frac{\text{wt}}{\text{Hz}\cdot\text{sr}}$$

According to (38), the spectral brightness of such OR source

$$B = 2.2 \times 10^{-7}\frac{\text{wt}}{\text{Hz}\cdot\text{cm}^2\cdot\text{sr}}$$

corresponds to the photon flux in the range of frequencies $d\omega/\omega_{1m} = 10^{-2}$ per unit area of a visible surface of the source.

$$\frac{dN}{dtdOdS} = 2.2 \times 10^{25}\frac{\text{photon}}{\text{S}\cdot\text{cm}^2\cdot\text{sr}}$$

This radiation is practically fully polarized. It is concentrated in a range of angles relatively to the ondulator axis.

$$\Delta\theta \simeq \frac{1}{\gamma}\sqrt{\vartheta_b^2 + (1 + P_\perp^2)\frac{d\omega}{\omega_{1m}}} \simeq 4 \times 10^{-5}$$

Note that the spectral-angular intensity of synchrotron radiation of the same beam from a bending magnet of the storage ring under consideration in the same spectral region[28] will be 5×10^3 times less.

4 OBSERVATION OF ONDULATORY RADIATION AT THE "PAKHRA" SYNCHROTRON

The installation of an ondulator into a straight section of an electron synchrotron or storage ring makes it possible to produce an intense OR in a wide spectrum range due to multiple travel of accelerated particles in the ondulator field (as follows from the previous section). However, up to date, the possibility of construction of such OR sources has not been yet investigated experimentally.

Below are presented some experiments to observe electron radiation in a magnetic ondulator installed in a straight section of the "Pakhra" synchrotron orbit.[39] The "Pakhra" synchrotron has the following parameters: maximum energy of accelerated electrons $E = 1.3$ GeV, bending radius of electron trajectory in magnetic field $R = 4$ m, number of straight sections 4, length of each section $l = 1.9$ m, frequency of betatron oscillations: $\nu_x = 0.785$; $\nu_z = 0.836$, beam intensity 10^{12} electrons/sec (corresponding to a circulating current $I \simeq 30$ mA), frequency of repetition of magnetic field cycles $f = 52$ Hz.

The experiment is schematically presented in Figure 6. The ondulator has 20 elements of periodicity. The length of each element is $\lambda_0 = 4$ cm. The magnetic field is produced by a single-turn flat coil containing an uneven number of series-parallel conductors oriented perpendicularly to the beam axis. The coil is located in grooves of the magnetic

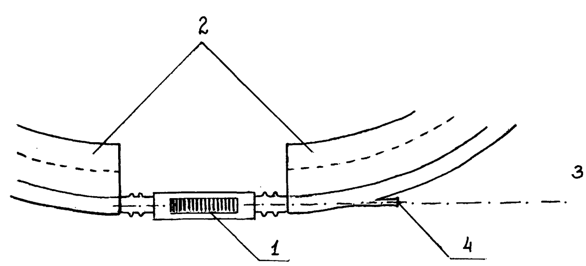

FIGURE 6 Layout of the experiment: 1—ondulator; 2—bending magnet of the accelerator; 3—photoplate; 4—quartz window.

conductor, made in the form of a ferromagnetic comb. The coil feeding is pulsed, the maximal current amplitude being 8 kA and the duration of a pulse being 2 to 3 nsec. The plane of the ondulator, facing the plane of equilibrium orbit, is spaced 25 mm from it. The amplitude of the transverse periodic magnetic field (4) H_m decreases with distance from the plane of the ondulator. To obtain the most effective generation of radiation, the beam should be as close as possible to the plane. Because of the reverse current conductor besides the transverse magnetic field, there is a vertically non-uniform constant component of radial magnetic field in this design. This causes a vertical displacement of the circulating beam.

The experiments were made with 3 kA in the ondulator coil. Under the experimental conditions, the vertical beam displacement on the azimuth was about 1 cm toward the ondulator. The amplitude of magnetic field $H_m = 0.036$ T corresponds to the given current and displacement of the synchrotron beam. In this case, the value $\alpha\gamma \sim 0.13$ meets the conditions of the dipole approximation (see Section 1). In this approximation, the radiation wavelength is plainly related to the electron energy and the observational angle

$$\lambda = \lambda_0/2\gamma^2(1 + \vartheta^2) \tag{42}$$

The photographic records of radiation were made by "spectral" plates type 2 with sensitivity from 5,000 Å to 2,000 Å. The photoplates were placed perpendicularly to the straight section axis at a distance of 440 cm from the ondulator center.

At a given period of ondulator $\lambda_0 = 4$ cm, the OR gets into the region of spectral sensitivity of photoplates beginning from the energy 100 MeV and above. The maximum electron energy was defined by the time of switching off high-frequency voltage on the accelerating resonator of the synchrotron. In addition, the pulsed magnetic field of the ondulator was energized. It reaches its amplitude value shortly before ($\sim$0.1 nsec) the switching off. This operation regime allows us to obtain the OR from almost monoenergetic electrons. To have OR in the optical wavelength range, the electron energy was varied in our experiments from 100 MeV to 175 MeV. The angular spread of particles in the beam was $\vartheta_n \simeq \frac{1}{2}\vartheta_n'$ in a given energy interval, arising to injection conditions and adiabatic damping. It slightly altered the spectral-angular distribution of radiation. In agreement with (42), at a maximum beam energy of 100 MeV we measured $\lambda(\theta = 0) = 5{,}000$ Å. The OR thus falls into a visible range, while the SR is in the infrared range outside the region of the photoplate sensitivity. A picture made in this experiment (Figure 7), shows that only ondulatory radiation is under observation. The size of the spot is mainly defined by the angular spread of particles in the beam and by the beam dimension. In agreement with the theory, photoplate blackening was not observed at lower energies. As the energy increases the SR appears in the visible spectrum range. In Figure 8(a) there is a photograph of synchrotron electron radiation with a maximum energy of 175 MeV (the ondulator being switched off). The left-hand band corresponds to the radiation at the distant (respective to the photoplate) quadrant output of the synchrotron chamber, while the right-hand one corresponds to the radiation at the near quadrant input. One can clearly see on the picture a minimum distribution

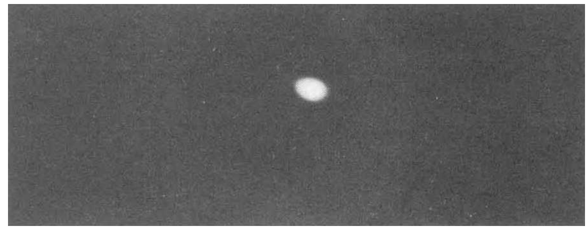

FIGURE 7 Photograph of ondulatory radiation. The energy is 100 MeV.

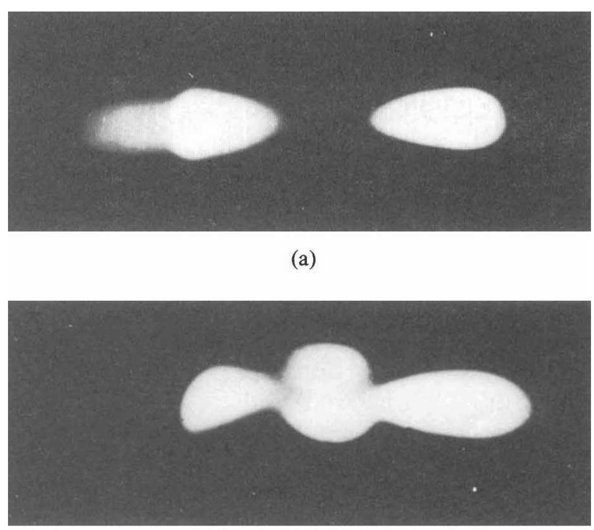

(a)

(b)

FIGURE 8 (a) Synchrotron radiation from bending magnets. The energy is 175 MeV. (b) Synchrotron and ondulatory radiation. The energy is 175 MeV.

of radiation intensity in the horizontal plane, corresponding to the beam axis in the straight section. The observed discontinuity in the bands may be accounted for by the fact that the electron radiation at a given energy in the fringing-field regions of a straight section (which noticeably moves the electron velocity vector) falls into the infrared range and is out of reach of the photoplates. A picture of the radiation of switched-on ondulator is given in Figure 8b. It shows that at the place of the minimum intensity of radiation of Figure 8a, a light spot is observed, which corresponds to electron radiation in the transverse periodic magnetic field of the ondulator. According to (42), the vertical size of the spot defined by the long-wavelength boundary of the photoplate sensitivity is in good agreement with the theory. The smaller intensity of blackening near the ondulator axis is due to $\lambda(\theta = 0) = 1700$ Å, which is out of the region of the spectral sensitivity of the photoplate. Note also that the intensity of ondulatory radiation in the particle-oscillation plane is weaker (see Figure 8b), because the angular distribution of electron radiation intensity here is characterized[23] by the presence of the two minima at an angle of $\theta = 1/\gamma$.

We should note that in our experiments the effective duration of SR exceeded duration of an OR pulse by about one order of magnitude. From a preliminary analysis of the photographs obtained, it follows that the OR intensity in a single interval of angle near the ondulator axis is several times higher than the corresponding SR intensity.

CONCLUSION

In this work, the basic features of the incoherent ondulatory radiation sources and ondulator types have been considered. Such sources, like SR ones, can be effectively used in investigations of solid spectroscopy, in molecular physics, in biology, photochemistry, and holography. They may be used as well as a spectrometric standard for laser pumping in the VUV and harder-spectrum regions.

Location of a helical ondulator in straight sections with colliding electron beams makes it possible to produce circularly polarized quasi-monochromatic photons of high energy.[34] Another means to get polarized quasi-monochromatic photons of high energy is utilization of a helical ondulator with monoenergetic electron beams obtained at the largest proton accelerators.[14] One may effectively use these ondulators for separating the electron beam from a hadron component[14] as well. The use of OR is also promising for the diagnosis of electron and proton beam behavior in synchrotrons and storage rings.[38,41]

REFERENCES

1. V. L. Ginsburg, *Izv. Akad. Nauk. SSSR, Ser. Fiz.*, **11**, 165 (1947).
2. H. Motz, *J. Appl. Phys.*, **22**, 527 (1951).
3. K. Landeker, *Phys. Rev.*, **86**, 852 (1951).
4. H. Motz *et al.*, *J. Appl. Phys.*, **24**, 856 (1953).
5. I. A. Grishaev *et al.*, *Dok. Akad. Nauk SSSR*, **131**, 61 (1960).
6. A. I. Alikhanyan *et al.*, *ZhETF Pis. Red.*, **15**, 142 (1972) [*JETP Lett.*, **15**, 98 (1972)].
7. R. Luis *et al.*, *Phys. Rev. Lett.*, **36**, 717 (1976).
8. D. F. Alferov *et al.*, Proc. III USSR National Conf. on Particle Accelerators, Moscow, I, 1973.
9. V. V. Anashin *et al.*, Proc. V USSR National Conf. on Particle Accelerators, annotation of works TZNII atom information, Moscow, 1976, p. 85.
10. G. Chu, Stanford Linear Accelerator Center SSRP Report No. 76/100 (1976).
11. D. J. Thompson, Proc. V USSR National Conf. on Particle Accelerators, annotation of works TZNII atom information, Moscow, 1976, p. 82.
12. E. M. Rowe *et al.*, Proc. V USSR National Conf. on Particle Accelerators, annotation of works TZNII atom information, Moscow, 1976, p. 83.
13. R. Chasman and G. K. Green, Proc. V USSR National Conf. on Particle Accelerators, annotation of works TZNII atom information, Moscow, 1976, p. 83.
14. D. F. Alferov *et al.*, *Pis'ma Zh. Tekh. Fiz.*, **2**, 487 (1976) [*Sov. Tech. Phys. Lett.*, **2**, 191 (1976)]; *Yad. Fiz.*, **27**, 971 (1978).
15. D. F. Alferov *et al.*, FIAN No. 23 (1972),
16. D. F. Alferov *et al.*, *Zh. Tekh. Fiz.*, **42**, 1921 (1972) [*Sov. Phys.-Tech. Phys.*, **17**, 1540 (1973)].
17. V. N. Baier *et al.*, *Zh. Eksp. Teor. Fiz.*, **63**, 2121) [*Sov. Phys.-JETP*, **36**, 1120 (1973)].
18. A. A. Sokolov *et al.*, *Zh. Tekh. Fiz.*, **43**, 682 (1973) [*Sov. Phys.-Tech. Phys.*, **18**, 430 (1973)].
19. D. F. Alferov *et al.*, *Zh. Tekh. Fiz.*, **43**, 2126 (1973) [*Sov. Phys.-Tech. Phys.*, **18**, 1336 (1974)].
20. V. G. Bagrov *et al.*, *Izv. Vyssh. Ucheb. Zaved. Fiz.*, No. 10, 50 (1973).
21. Yu. G. Pavlenko *et al.*, *Izv. Vyssh. Ucheb. Zaved. Fiz.*, No. 10, 88 (1973) [*Sov. Phys. J.*, **16**, 1411 (1973)].
22. A. Kh. Mussa *et al.*, Vestn. MGU, Fiz. Astron., No. 3 (1974).
23. D. F. Alferov *et al.*, FIAN No. 92 (1974); Trudy FIAN, *Synchrotron Radiation* (Nauka Press, Moscow, 1975) [*Synchrotron Radiation* (Ed. N. G. Basov) (Plenum, New York, 1975)].
24. A. B. Kukanov and G. A. Michurina, *Pis'ma Zh. Tekh. Fiz.*, **1**, 931 (1975) [*Sov. Tech. Phys. Lett.*, **1**, 402 (1975)].
25. D. F. Alferov *et al.*, FIAN No. 118 (1975); *Zh. Tekh. Fiz.*, **46**, 2392 (1976) [*Sov. Phys.-Tech. Phys.*, **21**, 1408 (1976)].
26. D. F. Alferov *et al.*, FIAN No. 163 (1976); *Zh. Tekh. Fiz.*, **48**, 1592 (1978).
27. V. L. Ginsburg, *Theoretical Physics and Astrophysics* [in Russian] (Nauka Press, Moscow, 1975).

28. A. A. Sokolov and I. M. Ternov, *The Relativistic Electron* [in Russian] (Nauka Press, Moscow, 1974).
29. V. V. Lebedeva, *Techniques of Optical Spectroscopy* [in Russian] (Moscow, 1977).
30. J. M. J. Madey, *J. Appl. Phys.*, **42**, 1906 (1971).
31. D. F. Alferov *et al.*, Proc. All-Union Conf. on Application and Use of Electron Accelerators, Tomsk, 1975, p. 214.
32. M. M. Nikitin and A. F. Medvedev, *Zh. Tekh. Fiz.*, **45**, 950 (1975) [*Sov. Phys.-Tech. Phys.*, **20**, 600 (1975)].
33. V. L. Ginsburg, Short Report on Physics, Trudy FIAN No. 2, 40 (1972).
34. Yu. A. Bashmakov and E. G. Bessonov, Proc. V USSR National Conf. on Particle Accelerators, annotation of works TZNII atom information, Moscow, 1976, p. 115.
35. M. A. Kumakhov, *Dokl. Akad. Nauk SSSR*, **230**, 1077 (1976) [*Sov. Phys. Dokl.*, **21**, 581 (1976)]; *Phys. Lett.*, **57A**, 17 (1976).
36. D. F. Alferov *et al.*, Proc. VIII USSR National Conf. on Physics of Charged Particle Interactions with Monocrystalline Particles, Moscow, MGU, 1976, p. 65.
37. M. M. Nikitin and V. Ya. Épp, *Zh. Tekh. Fiz.*, **46**, 2386 (1976) [*Sov. Phys.-Tech. Phys.*, **21**, 1404 (1976)].
38. D. F. Alferov and E. G. Bessonov, *Pis'ma Zh. Tekh. Fiz.*, **3**, 828 (1977) [*Sov. Tech. Phys. Lett.*, **3**, 336 (1977)].
39. D. F. Alferov *et al.*, *Pis'ma Zh. Eksp. Teor. Fiz.*, **26**, 525 (1977) [*Sov. Phys.-JETP Lett.*, **26**, 385 (1977)].
40. Wiggler Magnets (a collection of material presented at the Wiggler Workshop, SLAC, March 21–23, 1977, and other material related to wiggler magnets), edited by H. Winick and T. Knight, SSRP Report No. 77/05, May, 1977.
41. R. Coïsson, *Nucl. Instrum. Methods*, **143**, 241 (1977).